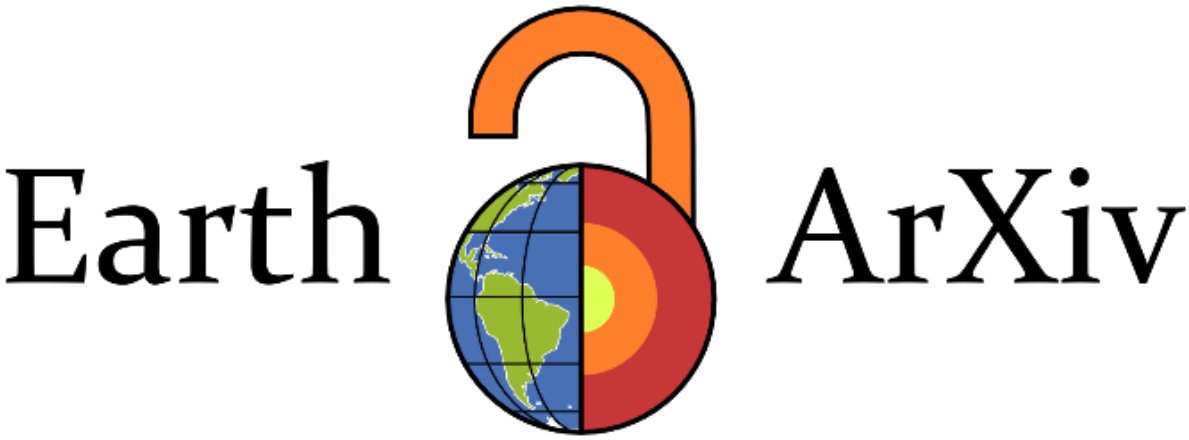

Peer review status:

This is a non-peer-reviewed preprint submitted to EarthArXiv.

Theory and Conditions for AI-Based Inversion Paradigm of Geophysical Parameters Using Energy Balance

Kebiao Mao[1,2*], Chenhao Wu[1], Zijin Yuan[1], Yangyang Liu[2], Mengmeng Cao[3,4], Han Wang[1]

[1]State Key Laboratory of Efficient Utilization of Arid and Semi-arid Arable Land in Northern China, Institute of Agricultural Resources and Regional Planning, Chinese Academy of Agricultural Sciences, Beijing, 100081, China.821012410306@caas.cn, Yuanzijin@caas.cn, 751218629@qq.com

[2]School of Electrical and Electronic-Engineering, Ningxia University, Yinchuan 750021, China. 3213529459@qq.com

[3]Key Laboratory of Geospatial Technology for the Middle and Lower Yellow River Regions (Henan University), Ministry of Education, Kaifeng 475004, China. mmengcao@henu.edu.cn

[4]College of Geography and Environmental Science, Henan University, Kaifeng 475004, China.

*Correspondence to: maokebiao@caas.cn

Tel.: +86-010-8210-8769

Declarations

Conflict of Interest:The authors declared that they have no conflict of interest.

Funding: Key Project of Natural Science Foundation of Ningxia Department of Science and Technology (No. 2024AC02032).

Acknowledgments: The authors would like to thank the NASA Earth Observing System Data and Information System for providing the MODIS data, the University Corporation for Atmospheric Research (UCAR) for providing Suominet Global Positioning System (GPS) site data, and the ECMWF for providing the fifth-generation climate reanalysis data.

Theory and Conditions for AI-Based Inversion Paradigm of Geophysical Parameters Using Energy Balance

Kebiao Mao[1,2*], Chenhao Wu[1], Zijin Yuan[1], Yangyang Liu[2], Mengmeng Cao[3,4], Han Wang[1]

[1]State Key Laboratory of Efficient Utilization of Arid and Semi-arid Arable Land in Northern China, Institute of Agricultural Resources and Regional Planning, Chinese Academy of Agricultural Sciences, Beijing, 100081, China.821012410306@caas.cn, Yuanzijin@caas.cn, 751218629@qq.com

[2]School of Electrical and Electronic-Engineering, Ningxia University, Yinchuan 750021, China. 3213529459@qq.com

[3]Key Laboratory of Geospatial Technology for the Middle and Lower Yellow River Regions (Henan University), Ministry of Education, Kaifeng 475004, China. mmengcao@henu.edu.cn

[4]College of Geography and Environmental Science, Henan University, Kaifeng 475004, China.

*Correspondence to: maokebiao@caas.cn

Tel.: +86-010-8210-8769

Abstract: To construct a universal artificial intelligence (AI) model for geophysical parameter inversion, this study proposes a new remote sensing parameter inversion paradigm theory by changing cognition to unify physical, statistics and AI methods. Using the energy balance equation, we demonstrate that establishing a closed system of physical inversion equations between input and output variables in deep learning is the foundation for forming parameter inversion paradigms. On this basis, a generalized statistical method is constructed to guide the acquisition of representative solutions required for deep learning, thereby achieving the coupling of physical and statistical methods. Meanwhile, paradigm judgment conditions can improve the accuracy of data collection. Theoretical derivation and experimental results indicate that deep learning achieves physical consistency and generalization in remote sensing parameter inversion. This theory lays the foundation for developing AI parameter inversion model based on energy balance, and can also optimize the design of remote sensing sensors.

Main Text: The integration of artificial intelligence (AI) into various industries is poised to drive the development of new technologies and products, fundamentally transforming human cognition and production processes, and significantly boosting social and industrial productivity[1,2]. Deep learning, one of the most crucial AI techniques, has sparked intense research interest in both academia and engineering, achieving notable success in natural language generation, computer vision, and speech recognition[3,4]. To advance AI, Yann LeCun, et al. have proposed and repeatedly emphasized that energy based models (EBMs) are a key direction for the future. EBMs represent a major shift in machine learning frameworks, grounded in physical and mathematical principles. The core concept of EBMs is to model a system's configuration based on its energy, minimizing the energy to find the optimal configuration or prediction[5,6]. Energy based models (EBMs) are currently mainly used in computer vision, natural language processing, generative modeling, anomaly detection, reinforcement learning, and medical image analysis. In visual and language tasks, evidence-based medicine helps to process complex data and generate realistic samples. However, training evidence-based medicine on high-dimensional data and large-scale scenarios is often slow and requires a significant amount

of computing resources. In addition, EBM is sensitive to hyperparameter selection and energy function design, which makes optimization challenging and limits their applicability in real-time applications and dynamic environments[7,8,9].

Remote sensing is one of the most ideal fields for applying energy based models (EBMs), as it essentially relies on the principle of energy balance. Current applications of remote sensing primarily use geometric radiative transfer within energy balance equations. Although AI methods are increasingly employed in remote sensing, a universal AI parameter inversion paradigm has yet to be developed. After over 20 years of research, we find that interpreting neural networks through quantum energy transfer and energy calculus can, under certain conditions, unify AI, statistical, and physical approaches, forming a general theoretical framework for AI-driven parameter inversion in remote sensing. In remote sensing, satellite sensors capture the quantum energy of targets to obtain target information. Initially, target-related physical parameters were identified through statistical regression by correlating sensor-captured energy data with ground measurements. To enhance accuracy and generalizability, researchers analyzed the factors influencing energy transmission, introduced more relevant variables, and refined physical mathematical models for greater precision and applicability. Neural networks have been used to further enhance accuracy by training input-output relationships for target information retrieval. However, in remote sensing, neural networks are frequently criticized as "black boxes" because they lack interpretability and physical significance. In the field of remote sensing research, physical methods are still the most widely accepted approach due to their adherence to current human understanding of logical physics deduction.

We rarely apply reverse thinking to analyze the intrinsic connections between statistical, physical, and artificial intelligence methods. However, if we reverse-engineer these methods, we will find that they are essentially consistent when some conditions are met. In thermal infrared remote sensing, researchers—consciously or unconsciously, use different cognitive frameworks at different scales to describe quantum energy from targets and obtain target information. These frameworks use different coordinate systems and mathematical methods to capture changes in energy information, thereby achieving target parameter information. The main difference between these methods lies in how they depict the spatial curve projection of target information. Statistical methods provide the most direct macroscopic perspective on quantum energy transfer, often ignoring potential relationships between details, dimensions, or variables, similar to one-dimensional or two-dimensional cognitive coordinate systems. In contrast, physical methods provide a more comprehensive perspective by defining relevant physical variables and considering the geometric transfer relationships of quantum energy transfer, similar to three-dimensional or multidimensional coordinate systems. However, due to the nonlinear behavior exhibited by most physical phenomena, these equations are typically more complex. Although physical methods have wider applicability, deriving analytical solutions often requires simplification, thereby reducing accuracy. Deep learning neural networks are different from the previous two methods because they are closer to the actual process of energy exchange and interaction of quantum energy in a more microscopic dimension. Neural networks approximate quantum level cognitive systems at the micro level, and the degree of approximation depends on advances in hardware technology. These three methods - statistics, physics, and artificial intelligence - represent a continuum of human cognition that spans the quantum coordinate system from macro to micro. At present, our main cognition and understanding are at the level of geometric and physical coordinate framework. In fact, the three methods are essentially the same, using different rulers to measure the same target.

Furthermore, from a mathematical perspective, the statistical method for thermal infrared remote sensing parameter inversion can be regarded as an approximate representation of the curve equation solved by physical methods. Similarly, deep learning neural networks approximate the solutions of physical methods through calculus because neural networks can approximate functions of any complexity[10]. In order to create a universal AI inversion paradigm theory for thermal infrared remote sensing, we propose coupling physics, statistics, and deep learning methods based on the principle of quantum energy radiation balance. Figure 1 shows the flowchart of AI coupled physical and statistical methods in thermal infrared remote sensing parameter inversion. This coupling improves the generalization, interpretability, and portability of AI based thermal infrared parameter inversion, providing a theoretical and technical foundation for AI remote sensing parameter inversion models based on energy balance. We use the energy balance equation as a basis to perform physical logical reasoning on the output and input variables of deep learning neural networks, in order to determine the factors that affect the output variables (parts a and A in Fig. 1). On the basis of physical logical reasoning, the logical relationship between the input and output variables in the AI parameter inversion model is determined by theoretically constructing a system of physical equations. This process determines how many input variables can uniquely determine the output variable (part b in Fig. 1). Next, we construct a generalized statistical method based on physical methods (part c in Fig. 1), and use multi-source data to obtain representative solutions for both physical and statistical methods (parts B and C in Fig. 1). These solutions are used as training and testing data for deep learning, achieving seamless integration of the three methods without the need to embed physical methods into neural networks, thus establishing a physically meaningful and interpretable general paradigm for AI inversion of remote sensing parameters. In addition, under the judgment conditions of paradigm theory, neural networks can also correct low-precision solutions (B and C), as these solutions are expected to align with the curve of physical methods, and neural networks are capable of approximating any complex curve. If some of the collected multi-source data deviates from this solution curve, the corresponding values can be refined through repeated training and fine-tuning to minimize the overall error and correct the relevant data.

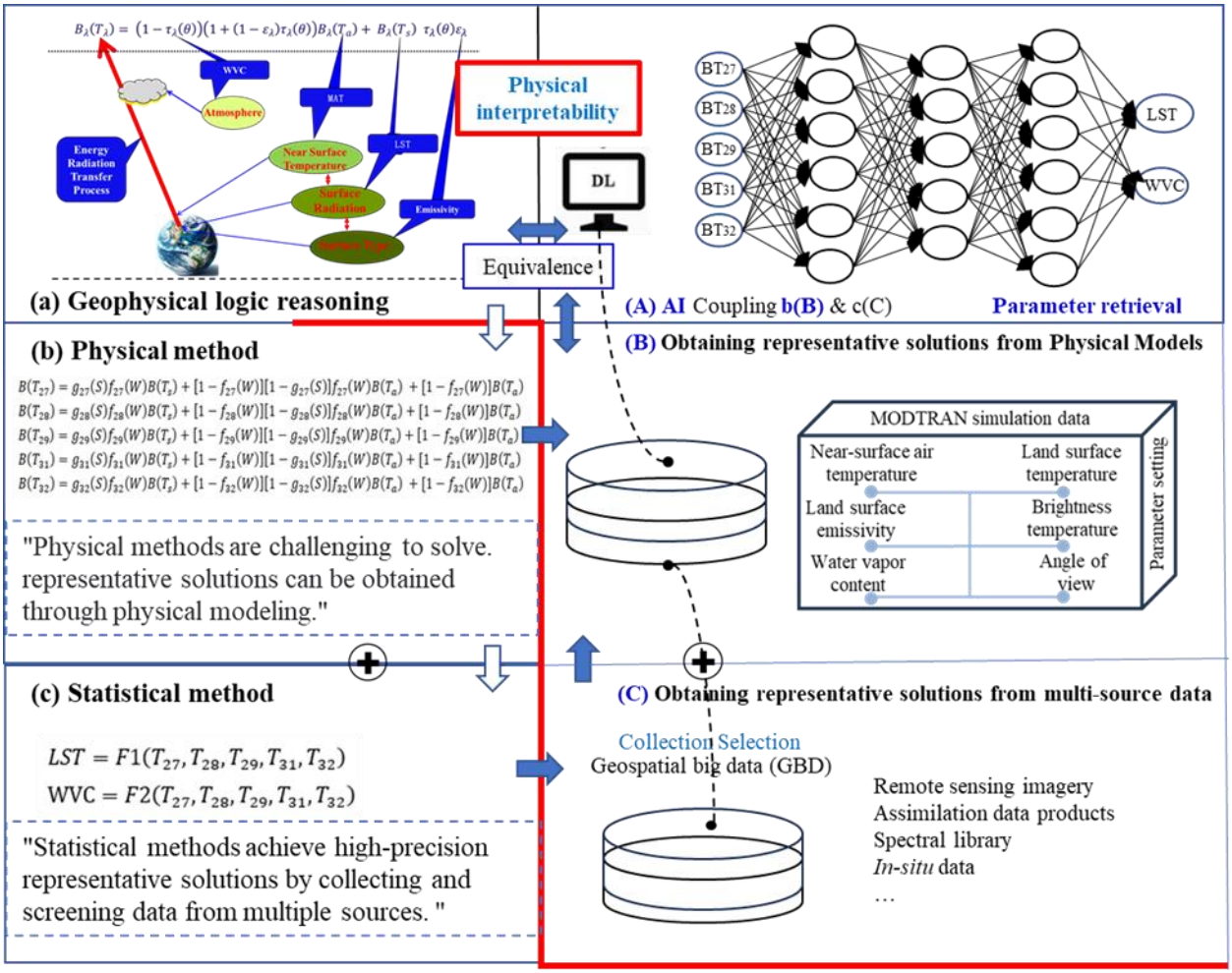

Fig.1. Flow chart of AI coupled physical and statistical methods for thermal infrared remote sensing parameter inversion. (a) Physical logic reasoning based on energy balance between input and output variables in deep learning networks; **(b)** Physical methods based on logical reasoning; **(c)** Generalized statistical methods based on physical methods; **(A)** Deep learning couples physical and statistical methods by using their solutions as training and testing data; **(B)** Obtaining representative solutions of physical methods through high-precision physical models; **(C)** Obtaining representative solutions of generalized statistical methods through multi-source data.

Results

Proof of AI Inversion Paradigm Theory and Conditions for Remote Sensing Parameters Based on Energy Balance

(1) Coupling analysis results of deep learning and physical methods

We utilize the inversion of thermal infrared remote sensing parameters, specifically land surface temperature (LST) and atmospheric water vapor content (WVC), to validate the AI parameter inversion paradigm theory. In the Supplementary Materials (S2.1-S2.5), we first conduct physical logical reasoning based on the radiative energy balance equation. Our analysis reveals that there are five unknowns affecting the deep learning output variables, corresponding to the five unknowns in the radiative transfer equation. Since three of these parameters are interdependent, one unknown can be reduced. Thus, to uniquely determine the output variables,

at least four radiative transfer equations must be constructed, implying that four input variables (brightness temperatures from four thermal infrared bands) are required as input for deep learning. According to our physical reasoning, when the number of input nodes in the deep learning neural network is fewer than four brightness temperatures from thermal infrared bands, the inversion accuracy decreases, or instability occurs.

We employed a fully connected deep learning neural network (10) and simulated data to invert land surface temperature (LST) and atmospheric water vapor content (WVC). Table 1 lists the theoretical inversion accuracies for LST and WVC using MODIS bands 27, 28, 29, 31, and 32 under different combination conditions. As shown in Table 1, the highest inversion accuracy is achieved when using the five-band combination (27, 28, 29, 31, 32), with a mean inversion error of 0.41 K for LST and 0.02 g/cm² for WVC. For LST, the average inversion error increases to 0.54 K when using the four-band combination (28, 29, 31, 32). For WVC, the average error remains 0.02 g/cm² with the four-band combination (27, 28, 31, 32), but increases to 0.131 g/cm² when using the combination (28, 29, 31, 32). As the number of bands decreases further, the inversion errors increase rapidly. When using the three-band combination (29, 31, 32), the mean inversion error for LST rises to 1.09 K, and for WVC, it rises to 0.317 g/cm². With the two-band combination (31, 32), the mean error for LST is 1.44 K, and for WVC, it is 0.479 g/cm². Using only one band (32), the mean error for LST reaches 3.62 K, and for WVC, it reaches 0.963 g/cm². These results indicate that fewer bands lead to greater errors, especially when fewer than four bands are used, which corroborates the correctness of AI parameter inversion paradigm theory and physical logical reasoning in the Supplementary Materials (S2.1-S2.5). To achieve lower inversion errors and generalizable methods, at least four thermal infrared bands are required to construct the radiative transfer equation system. Furthermore, Table 1 shows that for WVC inversion, the four-band combination (27, 28, 31, 32) is more accurate than (28, 29, 31, 32), suggesting that including a water vapor absorption band in the thermal infrared spectrum improves WVC inversion accuracy. For LST inversion, the five-band combination improves accuracy by 0.13 K compared to the four-band combination, indicating that considering the observation angle as an unknown variable enhances accuracy. However, due to the constraints of Equation (6) in the Supplementary Materials, reducing the unknown angle has minimal impact on accuracy, which is consistent with our theoretical analysis.

Table 1 Statistical results of LST&MVC inversion from simulated data (sorted in descending order by number of bands)

Band combinations	**MAE**	**RMSE**	**SD**	**R**	**Symbol**
(a) re_LST vs. LST (K)					
5BT_to_LST (27,28,29,31,32)	0.41	0.51	0.51	0.999	A1
4BT_to_LST (28,29,31,32)	0.54	0.73	0.72	0.999	A2
4BT_to_LST (27,28,31,32)	0.55	0.79	0.78	0.998	A3
3BT_to_LST (29,31,32)	1.09	1.46	1.45	0.995	A4
2BT_to_LST (31,32)	1.44	1.89	1.89	0.992	A5
1BT_to_LST (32)	3.62	4.94	4.93	0.942	A6
(b) re_WVC vs. WVC (g/cm^2)					
5BT_to WVC (27,28,29,31,32)	0.02	0.03	0.03	1.000	B1
4BT_to_WVC (27,28.31.32)	0.02	0.03	0.03	1.000	B2
4BT_to_WVC (28,29,31,32)	0.131	0.215	0.215	0.987	B3
3BT_to_WVC (29,31,32)	0.317	0.471	0.471	0.934	B4

2BT_to_WVC (31,32)	0.479	0.653	0.653	0.870	B5
1BT_to_WVC (32)	0.963	1.156	1.156	0.484	B6

In theory, if the equations were completely closed, the inversion error should approach zero. The presence of inversion errors indicates that physical methods or models themselves are approximations. Furthermore, land surface temperature and atmospheric water vapor are influenced by multiple factors. In practice, when constructing thermal radiative transfer equations, the influence of other gases is generally treated as constant, with radiative transfer primarily governed by variations in atmospheric water vapor content. However, the concentrations of other atmospheric components also fluctuate slightly with changes in temperature and water vapor, which could affect the accuracy of parameter inversion. These small variations are typically neglected in physical methods, leading to minor errors. Inversion results confirm that these effects are minimal, and considering factors such as instrument noise, this error can be ignored. If traditional methods are used to approximate the physical equation system, no matter how sophisticated the approach, the inversion error will inevitably be amplified. Therefore, based on physical reasoning, coupling physical methods with deep learning is the correct approach. Under satisfying the condition of AI parameter inversion paradigm (1. There is a causal relationship between input variables and output variables; 2. A closed system of equations can be constructed between the output and input variables.), these two methods are equivalent. Deep learning offers the optimal means of approximating the curve functions of physical solutions.

(2) Coupling analysis results of deep learning, physical and statistical methods

We validated the correctness of the AI parameter inversion paradigm theory by using physical models to simulate and obtain physical method solutions as training and testing databases for deep learning. Here, we further utilize multi-source data to obtain solutions for physical and statistical methods, demonstrating the effectiveness of deep learning coupling physical and statistical methods. We use generalized statistical methods derived from physical methods as guidance to obtain relevant supplementary solutions from multi-source data. MODIS product quality control documents and ERA5 data were used as control conditions to collect high-precision brightness temperatures, surface temperature, and atmospheric water vapor content.

Although precision control conditions were applied during multi-source data collection, the collected data still contain certain errors, with errors significantly larger than those in the simulated data. Since the collected data satisfy the AI parameter inversion paradigm conditions, meaning they meet equation 12 in supplementary materials. Therefore, here we adopt fine-tuning techniques to repeatedly correct the errors in the LST and WVC collected data. The detailed results are shown in scatter density plots, and each subplot "A1-A6, B1-B6" in Fig. 2 corresponds to the different combinations (Symbol) in Table 1. "N" represents "n_neighbors", the number of neighboring points around the target. From the clustering pattern and accuracy evaluation metrics in the figure 2, it is clear that both the 5-band and 4-band combinations exhibit significantly high accuracy in the inversion of LST and WVC. When fewer than four bands are used, the inversion accuracy declines notably. The multi-source data inversion analysis demonstrates that the AI remote sensing parameter inversion paradigm theory is feasible. Additionally, applying paradigm conditions and fine-tuning techniques can enhance the accuracy of collected data, further improving AI parameter inversion accuracy.

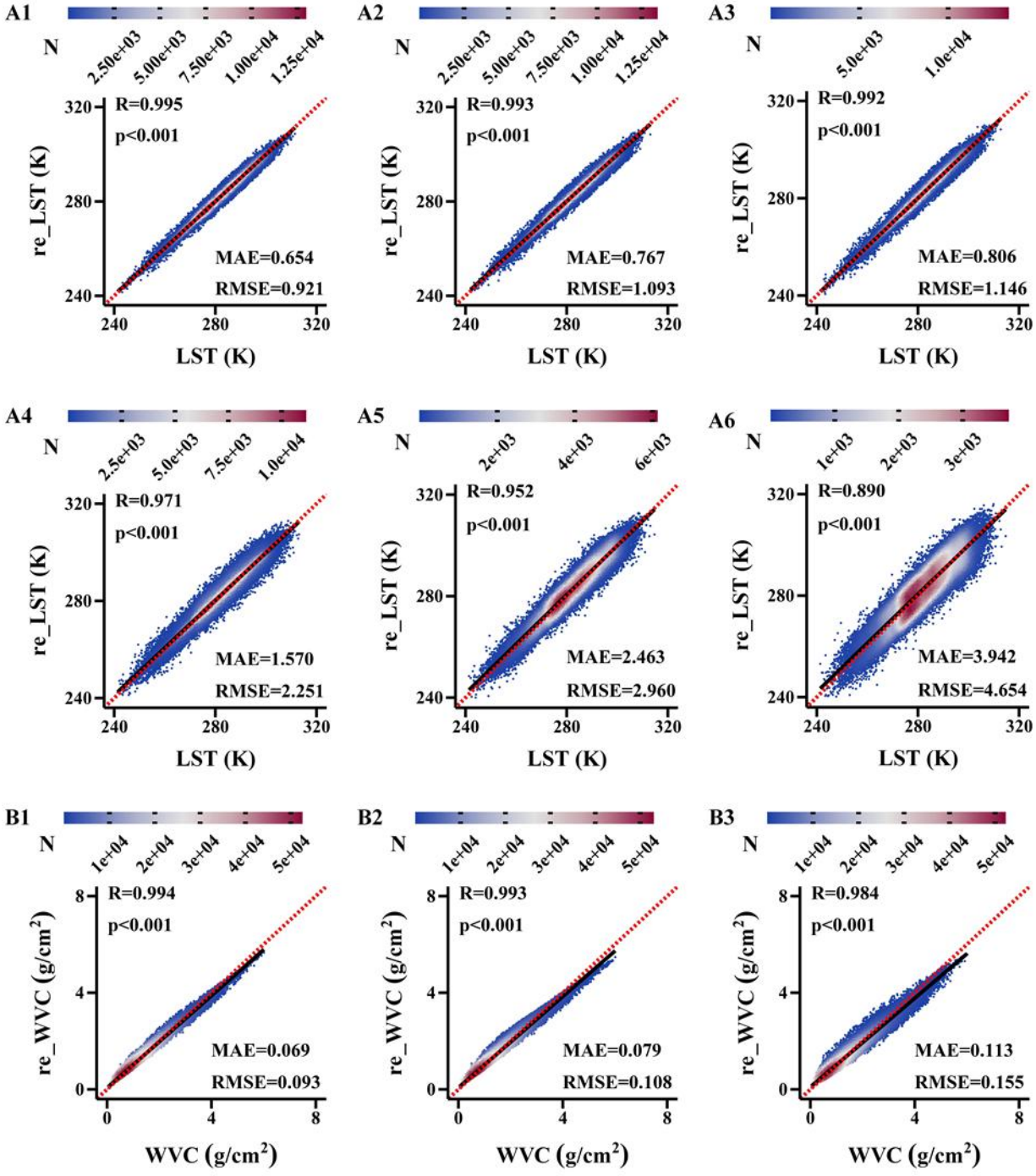
A1
N
2.50e+03
5.00e+03
7.50e+03
1.00e+04
1.25e+04
R=0.995
p<0.001
MAE=0.654
RMSE=0.921
re_LST (K)
LST (K)
A2
R=0.993
p<0.001
MAE=0.767
RMSE=1.093
A3
5.0e+03
1.0e+04
R=0.992
p<0.001
MAE=0.806
RMSE=1.146
A4
2.5e+03
5.0e+03
7.5e+03
1.0e+04
R=0.971
p<0.001
MAE=1.570
RMSE=2.251
A5
2e+03
4e+03
6e+03
R=0.952
p<0.001
MAE=2.463
RMSE=2.960
A6
1e+03
2e+03
3e+03
R=0.890
p<0.001
MAE=3.942
RMSE=4.654
B1
1e+04
2e+04
3e+04
4e+04
5e+04
R=0.994
p<0.001
MAE=0.069
RMSE=0.093
re_WVC (g/cm²)
WVC (g/cm²)
B2
R=0.993
p<0.001
MAE=0.079
RMSE=0.108
B3
R=0.984
p<0.001
MAE=0.113
RMSE=0.155

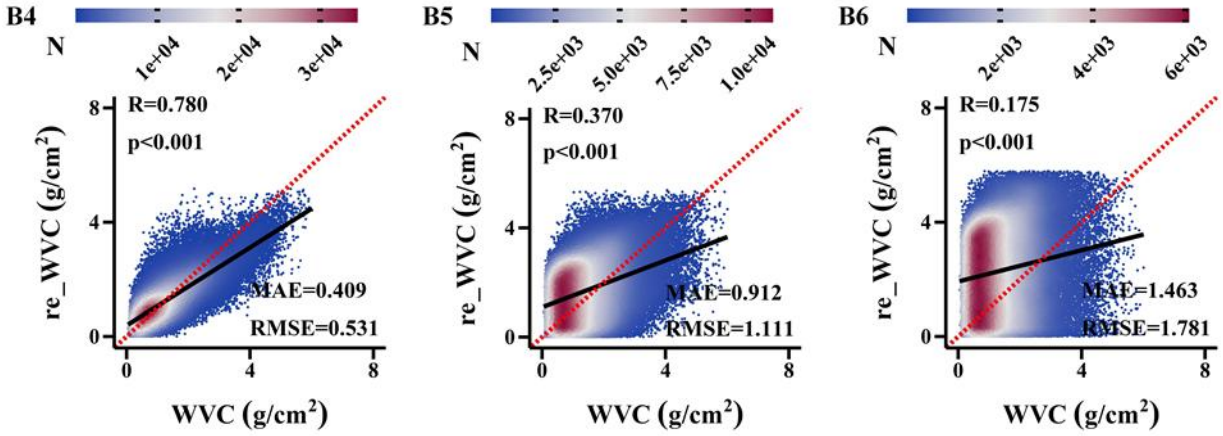

Fig. 2. Scatter density plot of the multi-source database results and validation for LST&WVC retrieval

（3）Ground observation station data validation

Finally, we validated the AI parameter retrieval paradigm theroy through ground observation stations. The validation results of LST and WVC are shown in Taylor Diagram (Figure 3). The diagram illustrates the performance differences and errors between the inversion values and the true values. Scatter points close to the true value (OBS) on the x-axis indicate smaller RMSEs, reflecting higher inversion accuracy. The distance from the origin represents the combined standard deviation (SD), while the radial lines indicate correlation coefficients. The results show that the average inversion accuracy of the five-band combination LST is about 0.816 K, and the correlation coefficient *R* is greater than 0.99. The average accuracy of the four-band combination LST is 0.923/0.985 K, with *R* exceeding 0.99. For WVC inversion, the average accuracy of the five-band combination is about 0.109 g/cm ², with *R* greater than 0.97, and the average accuracy of the four-band combination is 0.125/0.174 g/cm ², with *R* greater than 0.95. The verification of ground observation stations also confirms the correctness of the AI parameter inversion paradigm theory. The ground observation verification analysis also proves that the AI parameter inversion paradigm theory based on energy balance is correct.

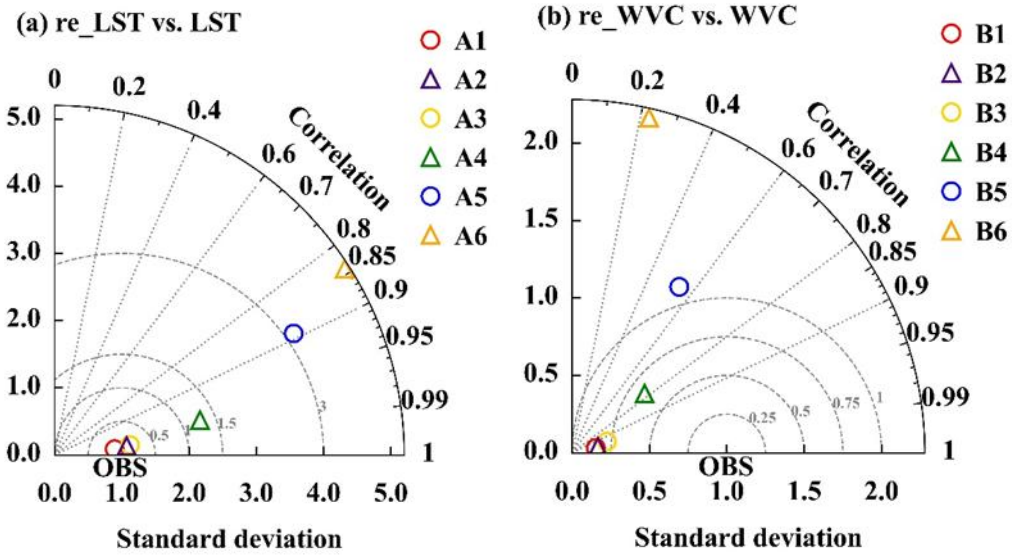

Fig. 3. Error Distribution Diagram of LST & WVC Retrieval and Validation Results at Observation Sites

This study analyzed the relationship between statistical methods, physical methods, and artificial intelligence (AI) technologies in thermal infrared remote sensing from both macro and micro cognitive perspectives. These methods use information of different granularities to describe the target, but they are essentially consistent.

To develop a large AI model for geophysical parameter inversion, **we propose an AI remote sensing parameter inversion paradigm theory based on energy balance and the basic conditions for determining the formation paradigm. Specifically, we first understand the information transmission mechanism of neurons in neural networks from a microscopic perspective of quantum energy transfer. Then, based on the energy radiation balance equation, we perform physical logical reasoning on the relationship between the input and output of AI method, proving that a closed inversion equation system can theoretically be constructed between the output and input variables of deep learning. This ensures that the output variable is uniquely determined by the input variable. On the basis of physical methods, we further constructed a generalized statistical approach to guide the extraction of representative solutions from multi-source data, which were then used as training and testing datasets for deep learning models. This perfectly couples artificial intelligence with physical and statistical methods.** In order to improve the accuracy of solutions obtained from multi-source data, we correct the collected data based on the judgment conditions and fine-tuning techniques of AI inversion paradigm. **The theoretical analysis and experimental results of thermal infrared remote sensing parameter inversion have demonstrated the feasibility of the theory and judgment conditions. Physical logical reasoning and experiments indicate that the conditions for forming an AI remote sensing parameter inversion paradigm based on energy balance are as follows: (1) In deep learning models, there is a causal relationship between input variables and output variables; (2) Prove that a closed system of physical equations can theoretically be constructed between the input and output variables of deep learning.** In fact, this is also an equivalent condition for the three methods of AI, physics, and statistics. Therefore, it is not necessary to embed physical methods into the neural network itself, but only to prove that the output variables in the neural network can be uniquely determined by the input variables. We conclude that this study provides a solid theoretical and technical foundation for constructing an AI model for remote sensing parameter inversion based on energy balance. **In addition, the analysis results can help optimize the band design of satellite remote sensors, which is a milestone in the development history of remote sensing parameter inversion.**

Discussion

Breakthroughs in artificial intelligence across various fields have driven the emergence of new technologies, products, and industries, fundamentally transforming human production, lifestyle, and thought processes, and elevating overall productivity. Changing cognitive frameworks is key to applying AI methods for high-precision retrieval of geophysical parameters. Statistical methods, physical methods, and AI approaches represent different cognitive coordinate systems that people have constructed—analogous to using different measurement scales for the same target information. While these three methods have traditionally been viewed as independent, they are, in fact, compatible when approached from a cognitive perspective of quantum energy balance. For remote sensing based on energy balance, statistical methods provide a macroscopic understanding of the target, physical methods offer a classical geometric

view of the world, and deep learning neural networks bring a quantum perspective, integrating quantum energy information to understand the world at a microscopic level. When the AI paradigm conditions are satisfied, these three methods become equivalent. With classical physical methods as a reference, statistical methods offer an abstract expression of the solution curve of physical methods, while deep learning utilizes representative solutions of physical and statistical methods to decompose relevant granularity information, and then integrates this information to approximate the solution curve function of physical methods.

Most people have not yet established the understanding of the process of energy transfer from a quantum perspective, and have not realized that deep learning can better approximate the real energy transfer process from a quantum dimension. To accurately identify targets, any method (statistical, physical, or AI) must satisfy energy balance or minimize energy loss. The improvement of cognition requires not only theoretical innovation, but also breakthroughs in the limitations of current hardware facilities such as computers and other hardware. In the future, the implementation and application of quantum computers and quantum remote sensing instruments will play an important role in improving human cognition. With the support of quantum computing and deep learning neural networks, human understanding of the world is expected to significantly improve. In theory, with the help of quantum computers, deep learning can gradually approximate the process of energy information transmission in the real world, and cognitive models that transmit information through quantum energy will eventually replace the current reliance on physical geometric models. This study combines three methods to elucidate the physical significance and universality of artificial intelligence methods, aiming to deepen our understanding of the current results. Essentially, what we need to do is to prove or confirm how many input variables are needed in deep learning to uniquely determine the output variables.

Main References

1 Hinton, G. E. Training products of experts by minimizing contrastive divergence. Neural Computation 14, 1771-1800, doi: 10.1162/089976602760128018(2002).

2. LeCun, Y., Bengio, Y. & Hinton, G. Deep learning. Nature 521, 436-444, doi:10.1038/nature14539 (2015).

3. Krizhevsky, A., Sutskever, I. & Hinton, G. E. ImageNet classification with deep convolutional neural networks. Advances in Neural Information Processing Systems 25, 1097-1105, doi: 10.1145/3065386(2012).

4. Bengio, Y., Ducharme, R., Vincent, P. & Janvin, C. A neural probabilistic language model. Journal of Machine Learning Research 3, 1137-1155, doi: 10.1162/153244303322533223(2003).

5. LeCun, Y., Bottou, L., Bengio, Y. & Haffner, P. Gradient-based learning applied to document recognition. Proceedings of the IEEE 86, 2278-2324, doi: 10.1109/5.726791 (1998).

6. LeCun, Y., Chopra, S., Hadsell, R., Ranzato, M. & Huang, F. A tutorial on energy-based learning. Predicting Structured Data 1, 1-59, doi: 10.7551/mitpress/9780262062694.003.0002(2006).

7. Teh, Y. W., Welling, M., Osindero, S. & Hinton, G. E. Energy-based models for sparse overcomplete representations. Journal of Machine Learning Research 4, 1235-1260, doi: 10.1162/153244303322533223(2003).

8. Nakamura, K., Yeung, S., Alahi, A. & Li, F.-F. Jointly learning energy expenditures and activities using egocentric multimodal signals. In Proceedings of the IEEE Conference on

Computer Vision and Pattern Recognition (CVPR), 1868-1877. doi: 10.1109/CVPR.2017.200 (2017).
9. Kim, T. &Bengio, Y. Deep directed generative models with energy-based probability estimation. In International Conference on Learning Representations (ICLR), doi: 10.48550/arXiv.1606.03439(2016).
10. Mao, K., Shi, J., Li, Z. & Tang, H. An RM-NN algorithm for retrieving land surface temperature and emissivity from EOS/MODIS data. Journal of Geophysical Research: Atmospheres 112, D21102, 1-17, doi: 10.1029/2007JD008428 (2007).

Methods:

1. Derivation of Theory

1.1 Theoretical Basis of AI Retrieval Paradigm in Thermal Infrared Remote Sensing

Thermal infrared remote sensing typically refers to the detection of terrestrial thermal radiation by infrared sensors on satellites or spacecraft. In the process of heat radiation from the Earth's surface to the satellite, energy transfer occurs through photon propagation. Photons, as quantum particles, possess quantized energy and momentum, meaning that the thermal energy emitted from the surface follows quantum mechanical principles throughout the transmission process[11-14]. Thermal infrared sensors detect energy by absorbing photons, which cause electron transitions. By measuring the number and energy of absorbed photons, sensors determine radiation intensity and spectral distribution, a fundamentally quantum process. According to Planck's law of black-body radiation, objects emit energy in the form of electromagnetic waves at any temperature, with these energies released as photons. The energy of each photon is quantized and proportional to its frequency, as described in Equation (1)[11]. This quantum relationship underpins the entire remote sensing process, from the surface emission to the sensor's photon detection, forming the theoretical foundation for the AI-based retrieval paradigm in thermal infrared remote sensing.

$$E = h\nu \qquad (1)$$

Here, E represents the photon energy, h is Planck's constant, and ν is the photon frequency. The Earth's surface primarily emits thermal energy in the form of infrared radiation, composed of infrared photons whose energy is also quantized. The frequency and wavelength of these photons are directly related to surface temperature. The quantized energy levels of photons, the quantum transitions in gas molecules, and the quantum detection by sensors all illustrate that this process is governed by quantum mechanics. Consequently, energy transfer is quantized, with each step involving absorption and emission of quantized energy. In the atmosphere, greenhouse gases (e.g., H2O, CO2, CH4) absorb infrared radiation at specific wavelengths, inducing energy-level transitions in these molecules. These absorption processes are quantized because gas molecules only absorb photons of specific energies, causing them to transition to higher quantum states. Upon returning to lower states, these gas molecules re-emit photons, whose energy remains quantized. From a microscopic quantum information transfer perspective, the exchange and transmission of quantized energy in thermal radiation are remarkably similar to the signal transmission in deep learning neural networks. However, due to limitations in hardware technology, the transmission of information between neurons in deep learning can be viewed as a mathematical calculus expression of microscopic quantum information. Physical methods can be seen as an integrative approximation, where neuron-like information is aggregated longitudinally and laterally to account for various factors affecting quantum information transfer, defined as relevant physical variables. Through simplification, these methods lead to the formulation of corresponding physical equations. Statistical methods, in turn, serve as a further integrative approximation of physical methods on a macroscopic scale, employing regression between target (dependent variables) and influencing factors (independent variables) to reveal patterns and relationships within the data. Therefore, these three approaches are inherently unified—they represent distinct cognitive frameworks constructed at different levels of granularity to achieve the same objective.

1.2 AI Physical Reasoning Based on the Energy Balance Equation

Due to the limitations of current computer hardware and the fact that classical physics is the main cognitive basis for solving problems, we use classical energy balance equations for physical logic reasoning to unify AI, physics, and statistics methods. The application of AI in remote sensing needs to be based on the background of specific problems. **When solving application problems, physical logical reasoning should take precedence over AI applications. We need to first determine which variables determine the output variables of deep learning, especially whether they can be uniquely determined by certain variables.** Therefore, before retrieving geophysical parameters, we must examine the inversion mechanisms of target parameters based on first principles. This involves clarifying, through physical reasoning, the underlying physical mechanisms that dictate which factors (variables) determine the outputs. The energy balance theory is the core of satellite remote sensing technology, emphasizing the balance between energy input and output in any system or process. Although energy transfer occurs in quantum form, current hardware and software limitations necessitate describing energy radiation processes using calculus, with further simplifications for practical application. The MODTRAN radiative transfer model simulates the process of integrated transfer of radiation energy information[15,16]. By dividing the atmosphere into 32 to 40 layers, MODTRAN performs physical simulations and mathematical calculations of the entire radiative process, ultimately integrating to produce simulated values. If the energy information flow is closed, then this process can be modeled by a deep learning neural network, rendering deep learning and MODTRAN models theoretically equivalent. Classical physical methods simplify MODTRAN's multi-layer atmospheric structure by defining equivalent (or integrated) variables to merge layers into a single approximation. Fundamentally, physical methods create a projection coordinate system that simplifies quantum-integrated information by defining variables, serving as a practical mathematical model for quantum information transfer. Thus, the physical method is effectively a simplified quantum information transfer model designed for easier application. MODTRAN is substantially more detailed than the simplified radiative transfer equations, and real quantum radiative transfer is, in turn, far more complex than MODTRAN. From the perspective of information transfer's underlying logic, deep learning, physical methods, and statistical methods are distinct mathematical characterizations that simplify the quantum information transfer process across different scales, from microscopic to macroscopic. The advantage of our AI parameter inversion paradigm theory is that as long as it is proven or determined that the output and input information of deep learning are closed, that is, theoretically a closed system of equations can be constructed, then the three methods (statistical, physical, and AI methods) can simulate the transmission process with any scale of information (training and testing data). This is similar to measuring the size of the Earth with a ruler in meters, centimeters, or nanometers. **As long as the hardware technology is advanced enough, the nanometer ruler (AI method) can replace or be equivalent to the centimeter ruler (physical method) and the meter ruler (statistical method).**

Thermal infrared remote sensing parameter retrieval is based on the thermal radiation energy balance equation. Extensive research has led to a simplified representation of the radiative transfer process[17], as shown in **Extended Data Fig. 1.** During the transmission of terrestrial thermal radiation through the atmosphere to the satellite sensor, key influencing factors include land surface temperature (LST), land surface emissivity (LSE), mean atmospheric temperature (MAT), and atmospheric water vapor content (WVC). The conduction of thermal radiation from the Earth's surface and its atmospheric transmission to the sensor can be represented by a classical energy balance equation, which is simplified as shown in Equation (2).

$$B(T_i) = \varepsilon_i \tau_i(\theta) B(T_s) + \left[1 - \tau_i\left(\theta^{'}\right)\right][1 - \varepsilon_i(\theta)]\tau_i(\theta) B(T_a) + [1 - \tau_i\left(\theta^{'}\right)]B(T_a) \quad (2)$$

In Equation (2), the left side represents the top-of-atmosphere radiance received by the satellite sensor, while the right side includes two main terms: the surface radiance and the atmospheric radiance contribution. Here, $B(T_i)$ denotes the radiance received by the satellite sensor in the i-th thermal infrared band (a known quantity), $\tau_i(\theta)$ represents the atmospheric transmittance for the i-th band (an unknown quantity), T_s is the surface temperature (an unknown quantity), T_a is the mean atmospheric temperature (an unknown quantity), and ε_i is the surface emissivity in the i-th band (an unknown quantity). Each term in the equation includes the Planck function[17, 18], as shown in Equation (3).

$$B_i(T_i) = \frac{C_1}{\lambda^5 (e^{\frac{C_2}{\lambda T_i}} - 1)} \quad (3)$$

Where $C_1 = 2c^2h = 1.191 \times 10^8 (\mathrm{W \cdot m^{-4} sr\text{-}1 \mu m^{-2}})$, $C_2 = \frac{ch}{k} = 1.439 \times 10^4 (\mu \mathrm{m \cdot K})$. Where c is the speed of light, with a value of $3 \times 10^8 (\mathrm{m \cdot s^{-1}})$, h is the Planck constant, with a value of $6.63 \times 10^{-34} (\mathrm{J \cdot s})$, and k is the Boltzmann constant, with a value of $1.38 \times 10^{-23} (\mathrm{J \cdot K^{-1}})$. As shown in Equation (2), each band has a distinct emissivity and transmittance. If the transmittance and emissivity for each band are unknown, then no matter how many thermal infrared bands are used, the resulting system of equations remains unsolvable. In the case of thermal infrared bands, transmittance is primarily influenced by atmospheric conditions, with atmospheric water vapor content being the main variable affecting these changes, while other gases remain relatively stable. Therefore, the transmittance for different bands can be expressed as a function of atmospheric water vapor content, as shown in Equation (4).

$$\tau_i = f_i(W, O) \quad (4)$$

Here, W represents atmospheric water vapor content, meaning that the transmittance for all bands can be reduced to a single unknown variable, the atmospheric water vapor content. O denotes other relatively stable gases, which can be considered constants. The emissivity for each thermal infrared band varies. Early algorithms typically treated the emissivity of each band as an unknown. However, within the thermal infrared spectrum, the emissivity curve for each land cover type is relatively stable, indicating that the emissivity of each band is a function of surface type, as shown in Equation (5).

$$\varepsilon_i = g_i(S) \quad (5)$$

Here, S represents surface type, which reduces the emissivity across different bands to a single unknown variable (the surface type). Although the observation angle for each pixel in a thermal infrared remote sensing image is known in Equation (2), the surface—particularly the land cover within each pixel—is not flat. Therefore, the observation angle is an effective incidence angle that varies with each satellite overpass. Strictly speaking, the observation angle is also an unknown variable. Thus, Equation (2) contains five unknowns: surface temperature, emissivity (surface type), atmospheric water vapor content, mean atmospheric temperature, and relative observation angle. Additionally, since there exists an approximately linear relationship between mean atmospheric temperature, the atmospheric profile, near-surface air temperature, and the satellite's top-of-atmosphere brightness temperature, this constraint is represented in Equation (6).

$$T_a \approx A_1 + B_1 T_0 \quad (6a)$$
$$T_a \approx A_2 + B_2 T_i \quad (6b)$$

In Equation (6), $A1$ and $A2$ are constants, and $B1$ and $B2$ are coefficients. A constraint relationship exists between Ta, $T0$, and Ti, indicating that atmospheric variables between the surface and sensor can provide additional conditions to help eliminate one unknown. Research on traditional algorithms has also confirmed this analysis[8].

From the perspective of quantum energy information transfer, the process of thermal radiation essentially describes the energy interaction between the target object (surface features) and the atmospheric medium before reaching the sensor. Transmittance and emissivity are variables defined by humans to describe this interaction process. Fundamentally, transmittance represents the remaining fraction of energy after interacting with atmospheric water vapor and other gases before reaching the sensor, while emissivity characterizes an object's inherent emission capability. Thus, it is more accurate to directly represent these variables in terms of their energy interaction counterparts—atmospheric water vapor, other gases, and surface types. The quantum energy transfer from the surface, interacting with various gas molecules in the atmosphere, closely resembles the information transfer between neurons in deep learning. As such, deep learning can effectively model the entire energy information propagation process. Under the condition of satisfying the AI remote sensing parameter inversion paradigm theory, if quantum computers were available, deep learning could theoretically approach the true energy transfer interaction process with infinite accuracy. Therefore, with advances in hardware technology and shifts in cognitive frameworks, we are moving progressively toward understanding the world through quantum information and quantum dimensions.

1.3 Physical Methods Based on Logical Physical Reasoning

Traditional classical physics methods effectively approximate real processes by integrating quantum energy information. Due to variations in terrain and atmospheric profiles, radiative transfer models differ by region, introducing certain errors in these simplified physical models. As deduced from the logical reasoning and analysis of the physical energy balance equation in Section 1.2, the thermal radiation balance equation determining the output variables includes at least five unknowns: surface temperature, emissivity (surface type), atmospheric water vapor content, mean atmospheric temperature, and relative incidence angle. If potential constraints between these parameters are considered, the number of unknowns can be reduced to four. Thus, the fundamental requirements for retrieving surface temperature and water vapor content in thermal infrared remote sensing are: (1) at least three thermal infrared window bands and one thermal infrared water vapor absorption band, or (2) at least four thermal infrared window bands. Only when these conditions are met, a closed system of energy balance equations can be formed. Using MODIS bands 27, 28, 29, 31, and 32 as an example, we construct the radiative transfer equations 7 as follows.

$$B(T_{27}) = g_{27}(S)f_{27}(W)B(T_s) + [1 - f_{27}(W)][1 - g_{27}(S)]f_{27}(W)B(T_a) + [1 - f_{27}(W)]B(T_a) \quad (7a)$$
$$B(T_{28}) = g_{28}(S)f_{28}(W)B(T_s) + [1 - f_{28}(W)][1 - g_{28}(S)]f_{28}(W)B(T_a) + [1 - f_{28}(W)]B(T_a) \quad (7b)$$
$$B(T_{29}) = g_{29}(S)f_{29}(W)B(T_s) + [1 - f_{29}(W)][1 - g_{29}(S)]f_{29}(W)B(T_a) + [1 - f_{29}(W)]B(T_a) \quad (7b)$$
$$B(T_{31}) = g_{31}(S)f_{31}(W)B(T_s) + [1 - f_{31}(W)][1 - g_{31}(S)]f_{31}(W)B(T_a) + [1 - f_{31}(W)]B(T_a) \quad (7c)$$
$$B(T_{32}) = g_{32}(S)f_{32}(W)B(T_s) + [1 - f_{32}(W)][1 - g_{32}(S)]f_{32}(W)B(T_a) + [1 - f_{32}(W)]B(T_a) \quad (7d)$$

Each term in the above system of energy balance equations includes the Planck function, which makes solving even a binary system challenging without simplification. In the split-window algorithm, Taylor expansion is typically used to simplify and solve the equations (*7*), yet this approach introduces significant error at the approximation bounds. Additionally, simplifications are inherent in calculating transmittance using atmospheric water vapor content and emissivity using surface type, which further amplifies computational errors. For an energy

balance system with more than three unknowns and only three equations, achieving precise solutions becomes increasingly difficult, and errors introduced by simplification are often unsatisfactory. To obtain high-precision solutions, optimizing iterative computational methods is the best approach for solving such physical equations, but this requires representative solutions. For thermal infrared remote sensing, the MODTRAN physical model is mainly applicable to simulations of single, homogeneous pixels. Therefore, MODTRAN simulations can be used to derive solutions for the physical equation system.

1.4 Generalized Statistical Methods Based on Physical Approaches

Traditional statistical and physical methods are typically constructed independently. Statistical methods generally perform regression directly between dependent and independent variables. In thermal infrared remote sensing, statistical methods for retrieving surface temperature and atmospheric water vapor content are usually expressed as shown in Equation (8).

$$\mathrm{LST}=a_1\mathrm{T}_{27}+a_2\mathrm{T}_{28}+a_3\mathrm{T}_{29}+a_4\mathrm{T}_{31}+a_5\mathrm{T}_{32}+c_1 \quad (8a)$$

$$\mathrm{WVC}=b_1\mathrm{T}_{27}+b_2\mathrm{T}_{28}+b_3\mathrm{T}_{29}+b_4\mathrm{T}_{31}+b_5\mathrm{T}_{32}+c_2 \quad (8b)$$

Here, ai(i=1∼5), bi(i=1∼5) are coefficients for the brightness temperatures T27, T28, T29, T31, T32, c_i (i=1,2) are constants. In essence, the statistical curve of Equation (8) from traditional statistical methods can be viewed as an approximate statistical solution to the physical equation system (Equation 7). This approximate solution is relatively rough and leads to relatively large errors. However, if we consider their objectives, both methods aim to retrieve information of the same target, making it possible to unify them. If the expression of the statistical method is constructed to follow the curve expression of the physical solution, then the statistical method becomes an alternative approximation of the physical solution function. Conversely, the curve expression of the physical solution can also be viewed as a form of the statistical method. Although traditionally seen as independent, these methods are, in fact, equivalent in representing the same target information through two different approaches. In the early development of thermal infrared remote sensing for LST and WVC retrieval, statistical methods were commonly used, mainly by regressing the satellite brightness temperature directly against ground-based LST and WVC observations. Single-band statistical methods performed regression using one brightness temperature with corresponding LST or WVC observations, while two-band methods used two brightness temperatures, and multi-band statistical methods involved multiple thermal infrared brightness temperatures. Since early statistical methods relied on direct regression between dependent and independent variables, most coefficients in these methods were fixed. For example, it was often assumed that the difference between two bands could eliminate atmospheric effects [7]. However, atmospheric profiles vary across regions, and thus the coefficients in statistical methods should, in reality, be variable. This limitation reduces the portability and accuracy of traditional statistical methods. Unlike traditional statistical approaches, our statistical method here is essentially a generalized expression of the physical solution. In other words, the unknowns and knowns in the statistical method align with those in the physical method, forming a generalized expression of the physical equation solution, as shown in Equation (9).

$$LST = F1(T_{27}, T_{28}, T_{29}, T_{31}, T_{32}) \quad (9a)$$

$$\mathrm{WVC} = F2(T_{27}, T_{28}, T_{29}, T_{31}, T_{32}) \quad (9b)$$

In the above equation, LST and WVC represent surface temperature and atmospheric water vapor content, respectively, while T27, T28, T29, T31, T32 are the top-of-atmosphere brightness temperatures across different bands. Traditional statistical methods determine the

coefficients for each band by performing regressions on large datasets. However, the coefficients in this statistical method are nonlinear and variable. Here, there is no need to compute statistical coefficients for the brightness temperatures of different bands. Instead, we obtain the corresponding statistical solution by collecting multi-source data, which includes the brightness temperatures from at least four bands along with synchronized measurements of surface temperature and atmospheric water vapor content. In essence, this statistical solution derived from multi-source data is also a solution of the physical method, though not obtained by solving a physical equation system. Therefore, from a reasoning and application perspective, physical and statistical methods are unified. The MODTRAN model can simulate only pure pixels, and physical models typically yield representative solutions for physical methods. However, real surfaces—particularly in medium- to low-resolution remote sensing images—mostly consist of mixed pixels. These mixed pixels on real surfaces are nonlinearly composed of various land cover types, forming a three-dimensional structure far more complex than simulations. Thus, obtaining a larger number of representative statistical solutions through multi-source data becomes highly important.

1.5 Unified Deep Learning-Physical-Statistical Parameter Retrieval Approach

It is well-known that with sufficient representative solutions, Deep learning can theoretically approximate any curve function[18]. Therefore, using the representative solutions from physical and statistical methods as training and testing data for deep learning allows deep learning to infinitely approximate the curve function of the physical method's solution and the generalized statistical method. As illustrated in **Fig. 1** of the main txt, the inversion paradigm of coupling AI with physical and statistical methods can be described as follows: First, perform physical logical reasoning on input and output variables of deep learning to establish a theoretical physical method based on energy balance, demonstrating the existence of a unique solution curve. On this foundation, construct a generalized statistical method. Then, acquire representative solutions from the physical and statistical methods using multi-source data to create the training and testing datasets for deep learning, thereby unifying the three approaches within a deep learning neural network. In this context, deep learning not only serves as an optimized curve representation of the solutions from physical and statistical methods but also achieves a seamless integration of all three approaches, endowing the method with physical significance, interpretability, and transferability. The entire process is shown in Fig. 1 of the main txt.

Through unified derivation and analysis of AI, physical, and generalized statistical methods, we conclude that to achieve physically meaningful, interpretable, and transferable AI-based retrieval of geophysical parameters grounded in energy balance, two fundamental conditions must be met: (1) a causal relationship exists between input and output variables; (2) it can be shown that a closed system of equations can be constructed between the input variables (x) and output variables (y) in deep learning, where the number of unknowns does not exceed the number of equations, ensuring that output parameters are uniquely determined by input parameters. This relationship can be mathematically represented by Equation (10).

$$f(x, y) = 0 \qquad (10)$$

Here, $x=x1, x2, \ldots, xn$; $y=y1, y2, \ldots, ym$; and f represents a vector function composed of k equations. To ensure that output variables can be uniquely determined by the input variables, the condition $k \geq m$ must be met. In other words, to ensure that the application of deep learning holds physical significance, physical logical reasoning must first be conducted to determine the necessary number of input variables for the target information (output variables). To make the solution space curve (dependent variable) unique, a coordinate system with the same dimension

as the independent variable can be constructed. If the coordinate system's dimension is insufficient to form a closed system, the solution curve will lack uniqueness, leading to potential errors. In addition, the solutions of physical and statistical methods collected from multiple sources data should theoretically satisfy equation 10. However, in practical situations, it is sometimes difficult to guarantee that all collected data theoretically satisfies the physical equation system, which means that all data should be on the solution curve. Therefore, we can use formula 11 to set different thresholds (*th*) and repeatedly train and test the collected data through deep learning to improve the accuracy of the collected data.

$$f(x, y) < \mathrm{th} \qquad (11)$$

2. Verification of Theory

2.1 Proof of Physical Method-Deep Learning Coupling

We used fully connected deep learning neural networks to invert simulated data, which is not limited to specific neural networks. Any fully connected deep learning neural network can obtain similar conclusions. Table 1 in main txt and **Extended Data Fig. 2** presents the theoretical retrieval accuracy for surface temperature and atmospheric water vapor using MODIS bands 27, 28, 29, 31, and 32 under different band combinations. From Table 1 in main txt and **Extended Data Fig.** 2a and 2b, it is evident that the highest retrieval accuracy is achieved using all five bands (27, 28, 29, 31, 32), yielding an average retrieval error of 0.41 K for surface temperature and 0.02 g/cm² for atmospheric water vapor. For surface temperature, the average retrieval error with a four-band combination (28, 29, 31, 32) is 0.54 K, while for atmospheric water vapor, using a four-band combination (27, 28, 31, 32) maintains an average error of 0.02 g/cm². However, with the combination (28, 29, 31, 32), the error increases to 0.131 g/cm². When the number of bands is further reduced, retrieval errors increase rapidly. With three bands (29, 31, 32), the average retrieval error for surface temperature rises to 1.09 K, and for atmospheric water vapor, it reaches 0.317 g/cm². Using only two bands (31, 32), the average error for surface temperature is 1.44 K, and for atmospheric water vapor, it is 0.479 g/cm². When a single band (32) is used, the average errors reach 3.62 K for surface temperature and 0.963 g/cm² for atmospheric water vapor. This indicates that fewer bands result in greater error, especially when fewer than four bands are used, confirming the validity of Theory and Criteria for an AI-Based General Inversion Paradigm of Thermal Infrared Remote Sensing Parameters Using Energy Balance. To achieve low retrieval errors and ensure the generality of the retrieval method, at least four thermal infrared bands are necessary to construct the retrieval radiative transfer equations. Additionally, Table 1 shows that for atmospheric water vapor retrieval, the four-band combination (27, 28, 31, 32) yields higher accuracy than the combination (28, 29, 31, 32), suggesting that including more water vapor absorption bands within the thermal infrared range improves retrieval accuracy. For surface temperature retrieval, the five-band combination provides a 0.13 K improvement over the four-band combination, indicating that considering angle as an unknown variable can further enhance accuracy. However, due to the constraints in Equation (6), reducing the angle as an unknown variable has minimal impact on accuracy, aligning well with theoretical analyses.

Theoretically, if the equations were fully closed, the inversion error should approach zero. However, the inversion analysis in Table 1 of main txt reveals a small residual error, indicating that the physical methods or models employed are also approximations. Surface temperature and atmospheric water vapor are influenced by multiple factors, while thermal infrared bands are primarily affected by atmospheric water vapor, other gases are approximately treated as constants. In reality, the concentration of other atmospheric components exhibits slight fluctuations with changes in temperature and water vapor content, which can subtly impact

retrieval accuracy. However, these minor variations are typically ignored in physical methods, leaving small residual errors. Evidence shows that these effects are indeed minimal and can be disregarded when considering factors such as instrument noise. If traditional approximation methods are used to solve the physical equation system, retrieval errors inevitably increase, regardless of the sophistication of the approach. These analyses indicate that the AI geophysical parameter inversion paradigm theory is correct, and if the output and input variables of deep learning satisfy the paradigm theory conditions, then deep learning and physical methods can be equivalent.

2.2 Proof of Deep Learning-Physical-Statistical Method Coupling

In this section, we use multi-source data to analyze the coupling of deep learning with physical and statistical methods. The accuracy of physical and statistical methods used for multi-source data collection directly affects the inversion accuracy of AI. In order to ensure the accuracy of multi-source data collection, we used the quality control files of MODIS products and data from ERA5 and other sources as control conditions. We collected 590,514 sets of corresponding satellite brightness temperatures, surface temperature, and atmospheric water vapor content data, which are representative solutions of statistical and physical methods. Although the product algorithms of MODIS LST and WVC have undergone about 15 years of research, data collection, algorithm development, and validation, forming the most stable MODIS LST and WVC products in the world[19,20,21], traditional physical algorithms mainly consider pure pixels, while most surface types are mixed pixels. Excessive or insufficient emissivity can lead to inversion errors in surface temperature products. Moreover, the validation of MODIS product data shows an accuracy of approximately ± 1 ° C under clear sky conditions and a single surface type. Due to factors such as atmospheric conditions, surface emissivity, and terrain complexity, MODIS temperature product errors may increase to 3-4 °C under complex terrain or high humidity conditions[22]. The accuracy of MODIS atmospheric water vapor products is usually between 10% and 15% under clear sky conditions, but cloud cover and aerosol concentration can increase the error of atmospheric water vapor inversion[23].

In order to further improve the accuracy of data collection, based on the AI parameter inversion paradigm theory and its judgment conditions, the collected data should satisfy the physical equation 7 and statistical method equation 9, that is, satisfy the paradigm judgment condition equation 10. From our analysis of the physical logic derivation of physical methods and the coupling between deep learning and physical methods, it can be seen that there are certain errors in the simplification of physical methods and the simulation of physical models. In addition, there are inevitably some systematic errors in sensors and ground observations. Therefore, we need to use formula 11 to set different thresholds and use deep learning to improve the accuracy of data collection. More representative solutions can be obtained under complex surface conditions and improve the inversion accuracy of complex terrain and mixed pixels. Deep learning is utilized to repeatedly train and stabilize the collected data, iteratively fine tune the collected data until the difference between the collected data and the output data satisfies the given condition in equation (12).

$$LST - F1(T_{27}, T_{28}, T_{29}, T_{31}, T_{32}) < 0.9 \quad (12a)$$

$$\mathrm{WVC} - F2(T_{27}, T_{28}, T_{29}, T_{31}, T_{32}) < 0.1 \quad (12b)$$

After fine-tuning to obtain stable collected data, the data was randomly divided into two parts, with 177,119 groups used as test data. **Fig. 2** in main txt and **Extended Data Table 1** show the

retrieval results for different band combinations of multi-source data, which demonstrate that the highest retrieval accuracy is achieved with five-band combinations, with average errors of less than 0.7 K and 0.07 g/cm2 for LST and WVC, respectively. When fewer than four bands are used, the error significantly increases, consistent with previous simulation data analysis, which further verifies the correctness of the AI parameter inversion paradigm theory and judgment conditions.

2.3 Cross-Validation of AI Retrieval Results with MODIS LST & WVC Products

To further verify the theory for an AI-Based General Inversion Paradigm of Thermal Infrared Remote Sensing Parameters, we conducted a cross-comparison between the multi-source data retrieval results and corresponding MODIS satellite LST and WVC products. Cross-validation results for different combinations are shown in **Extended Data Table 2**, **Extended Data Fig. 3.** and **Extended Data Fig. 4**. When using a five-band combination, the average inversion error of LST and WVC in cross validation is 0.867 K and 0.265 g/cm², respectively. When using a four-band combination, the average inversion errors of LST and WVC are 0.903/0.956 K and 0.303/0.357 g/cm², respectively. When the number of combined bands is less than 4, the analysis results are similar to the previous analysis results. Due to the relatively high error of MODIS products under complex surface conditions[22,23], some areas exhibit significant relative errors during cross validation. This highlights the advantages of the AI inversion paradigm based on deep learning: by fine-tuning the data to meet the conditions of the AI inversion framework (as analyzed in the previous section), we can improve the accuracy of sampled data and achieve higher parameter accuracy under complex conditions. Especially for atmospheric water vapor products, AI driven methods have great potential in improving inversion accuracy. Cross validation analysis shows that the paradigm theory of AI remote sensing parameter inversion is feasible.

2.4 Validation of LST & WVC with Ground Observation Stations

People usually use ground-based observational data to validate algorithms or theories. However, regardless of the accuracy of individual ground station measurements, due to variations in surface topography and atmospheric conditions, such measurements often fail to represent the true values of large-scale pixels. Therefore, we choose observation sites with flat terrain and uniform surface types as much as possible, and obtain observation data using auxiliary datasets (ERA5) as control conditions and MODIS 250-meter spatial resolution visible bands to confirm clear-sky conditions unaffected by clouds. we collected 775 sets of data, including MODIS brightness temperatures, surface temperature, and atmospheric water vapor. **Extended Data Table 3** and Fig. 3 in main txt present the retrieval accuracy for LST and WVC retrieval at ground observation stations. The retrieval accuracy for different band combinations was similar to the previous analyses. Results indicate that the five-band LST retrieval yields an average accuracy of approximately 0.816 K, with a correlation coefficient R exceeding 0.99. For the four-band combination, the average retrieval accuracy is 0.923/0.985 K, with R exceeding 0.99. For WVC retrieval, the five-band combination achieves an average accuracy of approximately 0.109 g/cm², with R exceeding 0.97, while the four-band combination provides an average accuracy of 0.125/0.174 g/cm², with R over 0.95. When the number of thermal infrared bands is less than 4, the verification of ground observation data is consistent with the previous analysis conclusion, indicating that the AI parameter inversion paradigm theory based on energy balance is correct.

At present, the AI geophysical parameter inversion method based on energy balance is still understood from the perspective of classical geometric physics energy transfer, rather than through the real process of quantum energy transfer. In order to maintain consistency with mainstream understanding of classical physics, we proposed that before applying artificial intelligence for geophysical parameter inversion, physical logical reasoning should be performed on the input and output variables of the artificial intelligence method to determine all factors that determine the output variables. On this basis, a physical method should be constructed. If physical methods cannot capture all the complexities of the real world, then a generalized statistical method based on physical methods should be further constructed to compensate for the shortcomings of physical methods. Then, representative solutions of physical and statistical methods can be obtained from multi-source data to construct deep learning training and testing databases, achieving seamless coupling and forming an AI parameter inversion paradigm theory based on energy balance. This ensures that AI methods have physical meaning, interpretability, and portability. The basic conditions for forming the paradigm of AI parameter inversion based on energy balance are: (1) there must be a causal relationship between input and output variables; (2) In theory, a closed system of equations can be constructed between the input and output variables of deep learning (with no more unknowns than the number of equations). If it can be proven that there is no closed relationship between input and output parameters (i.e. there are more unknowns than equations), then these applications may be limited to specific regions or have certain errors in the application process, lacking generalizability and portability, and therefore cannot be considered as paradigms.

In order to verify the correctness of the AI parameter inversion paradigm theory and judgment conditions based on energy balance, we used MODIS thermal infrared remote sensing data to invert surface temperature and atmospheric water vapor content as validation analysis. Through physical logical reasoning, it is shown that the inversion of thermal infrared remote sensing parameters requires five inversion equation sets, and the five bands of MODIS (27, 28, 29, 31, 32) are suitable for high-precision inversion of surface temperature and atmospheric water vapor. If considering the constraint relationship between parameters, although the accuracy slightly decreases when using a combination of four thermal infrared bands, it still meets the application requirements. We adopted multiple validation methods, including simulated data validation, multi-source database validation, cross validation with MODIS products, and ground station validation. These evaluations validated the feasibility of the artificial intelligence thermal infrared remote sensing inversion paradigm theory and judgment conditions from multiple perspectives. When fewer than 4 bands are used, the inversion accuracy rapidly decreases and becomes unstable, which supports the effectiveness of our proposed theory. In theory, using more thermal infrared window bands, especially those that include water vapor absorption, can achieve higher and more stable inversion accuracy, but this also increases computational time and hardware design complexity. Therefore, from a balanced perspective, the optimal sensor hardware design should include 3 thermal infrared window bands and 2 strong water vapor absorption bands, or 4 thermal infrared window bands and 1 strong water vapor absorption band. If there are difficulties in hardware design, ensuring 2 thermal infrared window bands and 2 strong water vapor absorption bands, or 3 thermal infrared window bands and 1 strong water vapor absorption band, can also achieve high-precision inversion of surface temperature and atmospheric water vapor content. Analysis confirms that the paradigm theory and conditions for geophysical parameter retrieval are robust, marking a milestone in applying artificial intelligence methods to geophysical parameter retrieval.

Methods References

11. Planck, M. On the Law of Distribution of Energy in the Normal Spectrum. Annalen der Physik 4, 553-563, doi: 10.1002/andp.19013090310(1901).
12. Dirac, P. A. M. The Quantum Theory of the Emission and Absorption of Radiation. Proceedings of the Royal Society A: Mathematical, Physical and Engineering Sciences 114, 243-265, doi: 10.1098/rspa.1927.0039 (1927).
13. Weisskopf, V. F. On the Theory of Radiation. Reviews of Modern Physics 7, 435-455, doi: 10.1103/RevModPhys.7.435(1935).
14. Feynman, R. P. Space-Time Approach to Quantum Electrodynamics. Physical Review 73, 318-356, doi: 10.1103/PhysRev.76.769(1948).
15. Berk, A. et al., MODTRAN5: A reformulated atmospheric band model with auxiliary species and practical multiple scattering options. Proc. SPIE 5806, 662-667, doi: 10.1117/12.606026(2005).
16. Berk, A. et al., MODTRAN6: A major upgrade of the MODTRAN radiative transfer code. Proc. SPIE 9088, 90880H, doi: 10.1117/12.2050433(2014).
17. Qin, Z. Dall'Olmo, G. Karnieli, A. & Berliner, P. Derivation of split-window algorithm and its sensitivity analysis for retrieving land surface temperature from NOAA-AVHRR data. Journal of Geophysical Research: Atmospheres 106, 22655-22670, doi: 10.1029/2000JD900452(2001).
18. Mao, K., Li, S., Wang, D., Zhang, L., Wang, X., Tang, H., & Li, Z. Retrieval of land surface temperature and emissivity from ASTER1B data using a dynamic learning neural network. International Journal of Remote Sensing 32, 5413–5423. doi:10.1080/01431161.2010.501043(2011).
19. Wan, Z. New refinements and validation of the MODIS Land Surface Temperature / Emissivity products. Remote Sensing of Environment 112, 59-74, doi: 10.1016/j.rse.2006.06.02(2008)6.
20. Coll, C. et al., Ground measurements for the validation of land surface temperatures derived from AATSR and MODIS data. Remote Sensing of Environment 97, 288-300, doi: 10.1016/j.rse.2005.05.007(2005).
21. Mieruch, S. et al., Comparison of water vapor column amounts derived from GOME and MODIS measurements. Journal of Geophysical Research: Atmospheres 113, D19, doi: 10.1029/2008JD010000(2008).
22. NASA MODIS Land Team, MODIS Land Surface Temperature Products Users' Guide. Available from: https://lpdaac.usgs.gov (2015).
23. NASA Goddard Space Flight Center (GSFC), MODIS Atmosphere Water Vapor Product Overview. Available from: https://modis-atmos.gsfc.nasa.gov (2020).

Acknowledgments: The authors would like to thank the NASA Earth Observing System Data and Information System for providing the MODIS data, the University Corporation for Atmospheric Research (UCAR) for providing Suominet Global Positioning System (GPS) site data, and the ECMWF for providing the fifth-generation climate reanalysis data.

Funding: Key Project of Natural Science Foundation of Ningxia Department of Science and Technology (No. 2024AC02032).

Author contributions: KM designed the research. KM, CW and ZY developed the methodology, and contributed to the results analysis and discussion. KM wrote the manuscript, and YL, MC and HW revised the manuscript.

Competing interests: The authors declare no competing financial interests.

Data and materials availability: All data used in this study are described in the Supplementary Materials, and all Python codes are available at http://.

Supplementary Materials

Supplementary Text

Materials

Tables S1

References

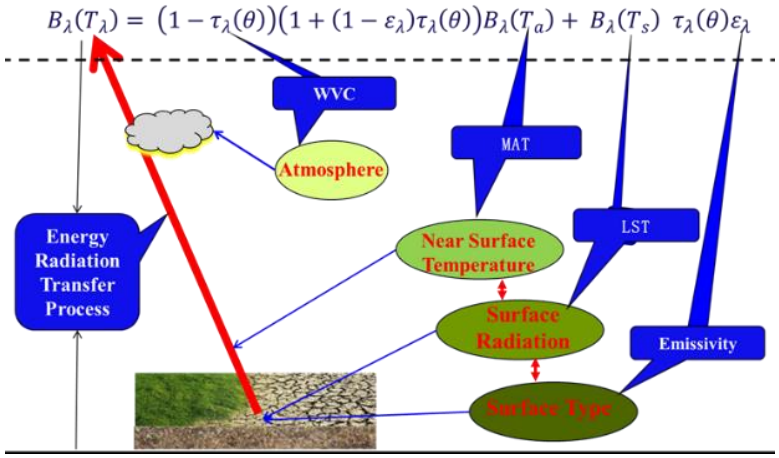

Extended Data Fig. 1. The relationship between agricultural meteorological remote sensing parameters (LST, LSE, MAT, WVC)

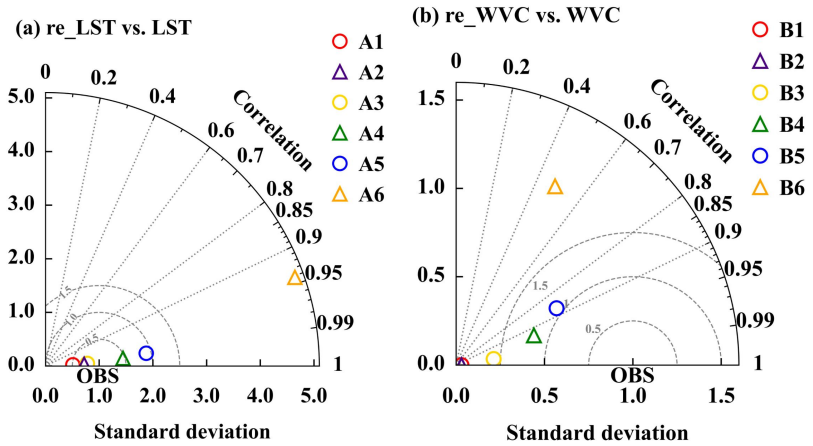

Extended Data Fig. 2. Error Distribution Diagram of LST and WVC Inversion Using Simulation Data

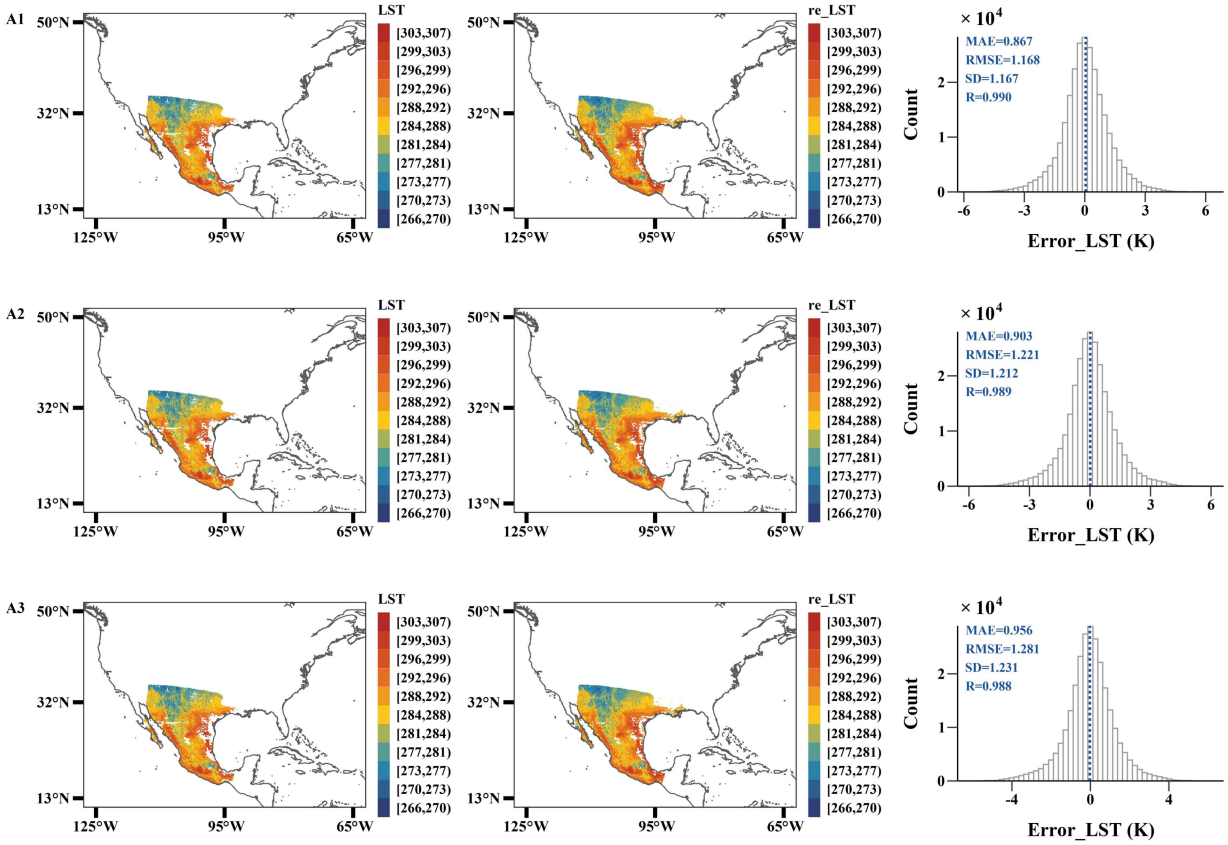

Extended Data Fig. 3. Cross-validation of MODIS LST products and MODIS retrieval LST result (2022.4.18) for band combination: (1) 5BT_to_LST（27, 28, 29, 31, 32）; (2) 4BT_to_LST（28, 29, 31,3 2）; (3) 4BT_to_LST (27, 28, 31, 32）. Histograms illustrate the statistical difference (MODIS LST product data minus MODIS retrieval LST data), in which the dashed blue lines represent the MAE.

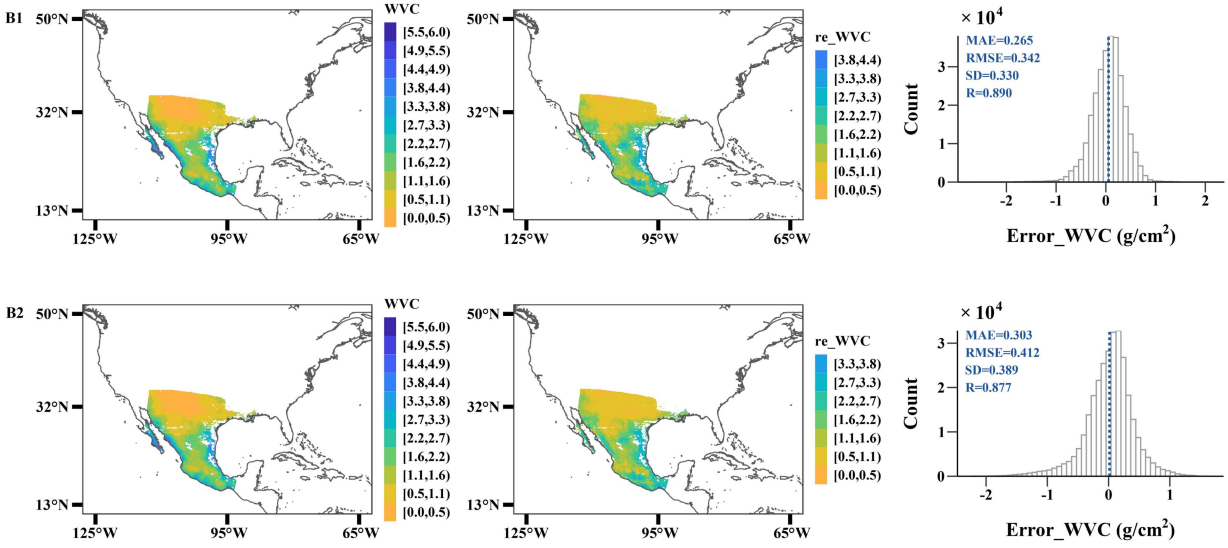

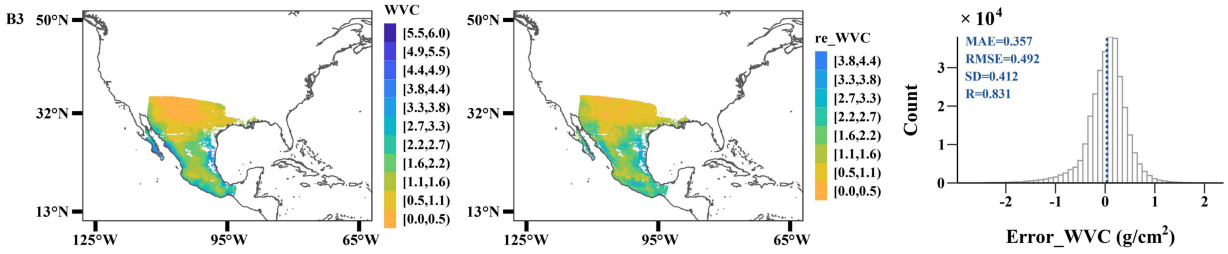

Extended Data Fig. 4. Cross-validation of MODIS WVC products and MODIS retrieval WVC result (2022.4.18) f or band combination: (1) 5BT_to_LST（27, 28, 29, 31, 32）; (2) 4BT_to_LST (27, 28, 31, 32）; (3) 4BT_to_LST （28, 29, 31,3 2）. Histograms illustrate the statistical difference (MODIS WVC product data minus MODIS retriev al WVC data), in which the dashed blue lines represent the MAE.

Extended Data Table 1. Statistical Results of Multi-Source Database Validation for LST & WVC Retrieval

Band combinations	MAE	RMSE	SD	R	Symbol
(c) re_LST vs. LST (K)					
5BT_to_LST（27,28,29,31,32)	0.654	0.921	0.921	0.995	A1
4BT_to_LST（28,29,31,32)	0.767	1.093	1.093	0.993	A2
4BT_to_LST (27,28,31,32)	0.806	1.146	1.145	0.992	A3
3BT_to_LST（29,31,32)	1.570	2.251	2.244	0.971	A4
2BT_to_LST（31,32)	2.463	2.970	2.927	0.952	A5
1BT_to_LST（32)	3.942	4.654	4.627	0.890	A6
(d) re_WVC vs. WVC (g/cm²)					
5BT_to WVC (27,28,29,31,32)	0.069	0.093	0.093	0.994	B1
4BT_to_WVC (27,28.31.32)	0.079	0.108	0.108	0.993	B2
4BT_to_WVC (28,29,31,32)	0.113	0.155	0.155	0.984	B3
3BT_to_WVC (29,31,32)	0.409	0.531	0.531	0.780	B4
2BT_to_WVC (31,32)	0.912	1.111	1.059	0.370	B5
1BT_to_WVC (32)	1.463	1.781	1.494	0.175	B6

Extended Data Table 2. Cross-Validation Statistical Results for LST & WVC Retrieval from Multi-Sour ce Database

Band combinations	MAE	RMSE	SD	R	Symbol
(a) re_LST vs. LST (K)					
5BT_to_LST（27,28,29,31,32)	0.867	1.168	1.167	0.990	A1
4BT_to_LST（28,29,31,32)	0.903	1.221	1.221	0.989	A2
4BT_to_LST (27,28,31,32）	0.956	1.281	1.281	0.988	A3
3BT_to_LST（29,31,32）	1.931	2.337	2.336	0.961	A4
2BT_to_LST（31,32）	2.985	3.532	3.513	0.918	A5
1BT_to_LST（32）	4.457	5.213	5.213	0.837	A6
(b) re_WVC vs. WVC (g/cm²)					
5BT_to WVC (27,28,29,31,32)	0.265	0.342	0.330	0.890	B1
4BT_to_WVC (27,28.31.32)	0.303	0.417	0.412	0.868	B2
4BT_to_WVC (28,29,31,32)	0.357	0.492	0.412	0.831	B3
3BT_to_WVC (29,31,32)	0.567	0.713	0.514	0.622	B4

2BT_to_WVC (31,32)	1.173	1.390	0.530	0.322	B5
1BT_to_WVC (32)	1.653	1.940	0.592	0.216	B6

Extended Data Table 3. Statistical Results of Ground Observation Station Validation for LST & WVC Retrieval from Multi-Source Database

Band combinations	**MAE**	**RMSE**	**SD**	**R**	**Symbol**
(a) re_LST vs. LST (K)					
5BT_to_LST（27,28,29,31,32）	0.816	1.017	0.897	0.995	A1
4BT_to_LST（28,29,31,32）	0.923	1.185	1.079	0.992	A2
4BT_to_LST (27,28,31,32）	0.985	1.261	1.130	0.991	A3
3BT_to_LST（29,31,32）	1.867	2.410	2.223	0.972	A4
2BT_to_LST（31,32）	3.222	4.207	3.989	0.891	A5
1BT_to_LST（32）	4.147	5.459	5.129	0.841	A6
(b) re_WVC vs. WVC (g/cm^2)					
5BT_to WVC (27,28,29,31,32)	0.109	0.156	0.156	0.978	B1
4BT_to_WVC (27,28.31.32)	0.125	0.171	0.171	0.973	B2
4BT_to_WVC (28,29,31,32)	0.174	0.236	0.236	0.950	B3
3BT_to_WVC (29,31,32)	0.447	0.605	0.604	0.774	B4
2BT_to_WVC (31,32)	0.965	1.290	1.276	0.542	B5
1BT_to_WVC (32)	1.652	2.257	2.219	0.224	B6

Supplementary Materials for

Theory and Conditions for AI-Based Inversion Paradigm of Geophysical Parameters Using Energy Balance

Kebiao Mao[1,2*], Chenhao Wu[1], Zijin Yuan[1], Yangyang Liu[2], Mengmeng Cao[3,4], Han Wang[1]

*Correspondence to: maokebiao@caas.cn

This PDF file includes:

Supplementary Text
Materials
Tables S1
References

Supplementary Text

Remote sensing technology is extensively applied in meteorology, agriculture, environmental monitoring, geological surveys, and other fields by providing high-resolution, large-scale data on dynamic changes within Earth's systems[1]. The fundamental principle of remote sensing involves the distant detection and acquisition of physical information of Earth's surface or atmosphere through sensors (such as those on satellites, drones, or aircraft) without direct touch with the target objects. Specifically, remote sensing relies on the unique properties of objects to reflect, absorb, or emit electromagnetic waves.The remote sensing process generally includes the following steps[2]: (1) Emission and Transmission of Electromagnetic Waves: Electromagnetic waves emitted by the sun or other radiation sources travel through the atmosphere to the Earth's surface, or, in active remote sensing (such as radar), are actively emitted by the sensors themselves. (2) Object Response: Earth's surface objects or atmospheric components (such as vegetation, water bodies, and soil) interact with electromagnetic waves according to their physical and chemical characteristics, reflecting, absorbing, or scattering the waves depending on their wavelengths. (3) Sensor Reception: Sensors mounted on satellites, aircraft, or drones receive these reflected or emitted electromagnetic signals and convert them into analyzable data (such as spectral information). (4) Data Processing and Analysis: Through computer processing of these signals, researchers can retrieve a range of information about the target objects, including surface temperature, atmospheric water vapor content, soil moisture, surface types, vegetation cover, terrain elevation, and more.

In the evolution of remote sensing technology, statistical methods, physical methods, and deep learning methods have each undergone distinct stages of development, progressively forming interrelated and complementary relationships[3-9]. (1)Statistical Methods: Statistical approaches were initially employed in remote sensing data processing, especially in early multispectral and thermal infrared remote sensing. By analyzing correlations between ground measurements and satellite observations, researchers used statistical regression techniques to establish simple empirical models for retrieving parameters such as surface temperature and water vapor content. Although statistical methods are straightforward and direct, they often overlook complex physical mechanisms, resulting in limited generalizability and accuracy, and their performance is sensitive to data variability. (2) Physical methods: With the advancement of remote sensing technology, physical methods have become the mainstream of inversion tasks. Based on the theory of energy radiation transfer, physical methods derive precise relationships between various physical processes through energy balance equations. Especially in thermal infrared remote sensing, physical models more accurately describe the energy transfer process between the atmosphere and the Earth's surface, providing higher inversion accuracy. However, these methods require intensive calculations and a large number of input parameters, often leading to errors due to insufficient observations and the need to supplement prior knowledge, such as thermal infrared remote sensing of surface temperature and atmospheric water vapor inversion. Moreover, solving complex equations often requires simplification, which can introduce errors. (3) Deep learning methods: Recently, with the improvement of computing power, deep learning methods have become prominent in remote sensing. Neural networks trained on massive remote sensing data can automatically learn complex nonlinear relationships between inputs and outputs, and can achieve local high-precision inversion without a clear physical model, lacking portability.

Traditionally, statistical, physical, and deep learning methods in remote sensing have been viewed as independent approaches. However, under certain conditions, these methods can be equivalent. This study demonstrates this equivalence by conducting a physical-logical reasoning of input and output variables within deep learning neural networks, thus constructing a physical method that proves how input variables uniquely determine output variables. Building upon this physical approach, a generalized statistical method is then developed. This generalized statistical method guides the acquisition of representative solutions for physical and statistical methods from multi-source data, which serve as training and testing data for deep learning. This integration achieves method coupling from macro to micro scales. In this study, we propose a paradigm theory for AI inversion of remote sensing parameters based on energy balance. This theory proves the existence of physical methods by performing physical logical reasoning on the input and output parameters of deep learning, and constructs generalized statistical methods based on this. Guided by this, representative solutions are obtained from multi-source data to form training and testing data for deep learning, thus achieving the coupling of AI with physical and statistical methods. The equivalent conditions of the three methods serve as the basic conditions for forming the AI remote sensing parameter inversion paradigm, and the construction of fine-tuning techniques to correct and improve the accuracy of collected data provides a theoretical and technical basis for establishing a universal AI model for remote sensing parameter inversion.

1 Materials

MODIS, mounted on the two polar-orbiting satellites Terra and Aqua, serves as a crucial sensor for observing global biological and physical processes and is part of the United States Earth Observing System (EOS) program, launched in 1999 and 2002, respectively. MODIS is particularly valuable due to its global coverage, radiometric resolution, and dynamic range, along with precise calibration in multiple thermal infrared bands, specifically designed for retrieving SST (Sea Surface Temperature), LST (Land Surface Temperature), and atmospheric properties. With spatial resolutions of 250 meters (0.62-0.876 μm), 500 meters (0.459-2.155 μm), and 1 kilometer (0.405-14.385 μm), and a scanning swath width of 1,330 kilometers, MODIS includes bands 27, 28, 29, 31, and 32 (6.53–11.28 μm) optimized for retrieving land surface temperature and atmospheric water vapor content, with mature LST and WVC (Water Vapor Content) products [10-12]. As one of the most advanced sensors with the highest quantity and quality of thermal infrared bands available, MODIS was selected in this study, specifically bands 27, 28, 29, 31, and 32 (6.53–11.28 μm), to validate and analyze the AI-based parameter retrieval paradigm theroy. Among these, bands 27 and 28 fall within the strong water vapor absorption range of the thermal infrared spectrum, while bands 31 and 32 are within the thermal infrared window region.

(1) Simulated Data

MODTRAN, a widely used medium-spectral-resolution radiative transfer model, simulates the entire radiative transfer process by configuring various surface, atmospheric, and instrumental parameters[13,14]. In this study, land surface temperature (LST) and atmospheric water vapor content (WVC) are the target parameters for the physical method (solutions of the equations). By setting different conditions such as surface temperature, surface type, and atmospheric profiles, we obtained representative simulated data for each MODIS thermal infrared band, thus yielding the representative solutions for the physical method. Key parameters include: (1) Surface Type (Emissivity): 17 surface types were selected, including soil, vegetation, water, and rock; (2) Surface Temperature: Training data range from 282 to 326K with a step size of 2 K; test data

range from 281 to 323K with a step size of 3K; (3) Atmospheric Water Vapor Content: Training data range from 0.2 to 3.4 g/cm² with a step size of 0.3 g/cm²; test data range from 0.2 to 3.4 g/cm² with a step size of 0.4 g/cm²; (4) Satellite Observation Angle: Varied from 0° to 65° with a step size of 3°. By setting weather modes and various model parameters, we obtained brightness temperatures for MODIS thermal infrared bands 27, 28, 29, 31, and 32 under specific weather conditions. Observations with excessive angles were excluded due to low transmittance caused by increased water vapor along the slant path. The calculated results include onboard brightness temperatures for each band, as well as the true values of the set surface temperature and atmospheric water vapor. The simulated data were divided into two parts: 195,000 sets for training and 39,000 sets for testing.

(2) Remote Sensing Data

The MODIS Land Surface Temperature (LST) and Water Vapor Content products were developed and produced by NASA's Goddard Space Flight Center (GSFC) and its scientific teams. Initiated in the early 1990s, this project aimed to provide high temporal and spatial resolution remote sensing data for global environmental and climate change monitoring[15, 16]. Following the successful launches of the Terra (1999) and Aqua (2002) satellites, the MODIS sensor began collecting data. After approximately 15 years of research, data acquisition, algorithm development, and validation, NASA released the stable MODIS LST and Water Vapor Content products around 2005 [10,17,18]. Under clear-sky conditions, the theoretical accuracy of MODIS LST products is approximately ±1°C. However, due to factors such as atmospheric conditions, surface emissivity, and terrain complexity, errors can increase to 3–4°C in areas with complex topography or high humidity[11,19]. The accuracy of the MODIS Water Vapor product generally falls within 10–15%, performing best under clear atmospheric conditions, though increasing cloud cover and aerosol concentrations may affect the precision of water vapor measurements[12,20]. For this study, we selected MOD/MYD021KM, MOD/MYD11_L2, and MOD/MYD05 data (Table 1) under clear-sky conditions for the United States and China from 2017 to 2022. Through product quality control files, we collected 590,514 sets of corresponding onboard satellite brightness temperatures, surface temperature, and atmospheric water vapor content data—representative solutions for the statistical and physical method.

Table S1. Satellite Remote Sensing Data and Related Products

Variable	Dataset	Resolution	Data Source
Brightness Temperature (BT)	MOD/MYD021KM	0.01°/5 minutes	https://ladsweb.modaps.eosdis.nasa.gov/search/
Land Surface Temperature (LST)	MOD/MYD11 L2	0.01°/5 minutes	
Atmospheric Water Vapor (WVC)	MOD/MYD05	0.05° /day	https://ladsweb.modaps.eosdis.nasa.gov/search/

(3) Ground-Based Observations and Assimilated Data

Ground-based observational data primarily come from monitoring stations in the United States and China. The U.S. Surface Radiation Budget Network (SURFRAD), established in 1993, aims to support climate research by providing precise, continuous, and long-term measurements of surface radiation across the U.S. [21]. Operational since 1995 with an initial four sites, SURFRAD now includes eight stations across diverse U.S. climate regions. Key measurements include

upward and downward components of solar and infrared radiation, with additional observations of direct and diffuse solar radiation, UV-B radiation, and meteorological parameters. Located in rural areas, SURFRAD stations offer unique in situ LST information, widely used to validate satellite-based LST retrievals. For atmospheric water vapor content (WVC) retrieval, data from AERONET stations were used. These measurements come from the AERONET (https://aeronet.gsfc.nasa.gov/) network, which employs sun photometers to achieve high precision and consistency across different sites. Additionally, this study incorporates hourly LST and WVC data from 2,399 meteorological stations in China from 2003 to 2022, provided by the China Meteorological Administration (CMA, http://data.cma.cn/), which undergo strict quality control and evaluation. To ensure accuracy in the alignment of ground-based observation data with MODIS data, ERA5 data and atmospheric water vapor data from the Suominet network were also employed. ERA5 is the fifth-generation global atmospheric reanalysis dataset, developed by the European Centre for Medium-Range Weather Forecasts (ECMWF)[22,23], covering data since 1940. ERA5 was built from ERA-Interim data, integrating model and global observational data to produce a coherent dataset. It provides hourly surface temperature and atmospheric water vapor data with a spatial resolution of 0.25°, and numerous studies have validated its accuracy since releaseing algorithms largely depends on the quality of training and test data. To ensure data accuracy, ERA5 was used as a reference calibration dataset, and only data products with consistent accuracy were included in the training and testing of the deep learning model. The Suominet network provides real-time atmospheric water vapor data derived from the National Global Positioning System (GPS) Network, established across North America and globally, totaling approximately 800 stations. Each station provides atmospheric water vapor data every 30 minutes with an accuracy of 1–2 mm[24].

References

1. Goetz, S. J., Prince, S. D. & Small, J. Advances in satellite remote sensing of environmental variables for epidemiological applications: A review. Remote Sensing of Environment 76, 245-256, doi: 10.1016/S0034-4257(01)00149-0 (2000).
2. Schowengerdt, R. A. Remote Sensing: Models and Methods for Image Processing. 3rd ed., Academic Press, doi: 10.1016/B978-0-12-369407-2.X5000-0(2007).
3. Becker, F. & Li, Z. L. Temperature-independent spectral indices in thermal infrared bands. Remote Sensing of Environment 32, 17-33, doi:10.1016/0034-4257(90)90095-4(1990).
4. Li, Z.-L. et al., Satellite-derived land surface temperature: Current status and perspectives. Remote Sensing of Environment 131, 14-37, doi: 10.1016/j.rse.2012.12.008 (2013).
5. Jackson, R. D. & Schmugge, T. J. Vegetation effects on the microwave emission of soils. Remote Sensing of Environment 36, 203-212, doi: 10.1016/0034-4257(91)90057-D (1991).
6. Lu, D. & Weng, Q. A survey of image classification methods and techniques for improving classification performance. International Journal of Remote Sensing 28, 823-870, doi: 10.1080/01431160600746456 (2007).
7. Qin, Z. Dall'Olmo, G. Karnieli, A. & Berliner, P. Derivation of split-window algorithm and its sensitivity analysis for retrieving land surface temperature from NOAA-AVHRR data. Journal of Geophysical Research: Atmospheres 106, 22655-22670, doi: 10.1029/2000JD900452(2001).

8. Mao, K., Shi, J., Li, Z. & Tang, H. An RM-NN algorithm for retrieving land surface temperature and emissivity from EOS/MODIS data. Journal of Geophysical Research: Atmospheres 112, D21102, 1-17, doi: 10.1029/2007JD008428 (2007).
9. Wang H. et al., A method for land surface temperature retrieval based on model-data-knowledge-driven and deep learning. Remote Sensing of Environment 265, 1-19, doi: 10.1016/j.rse.2021.112665(2021).
10. Wan, Z. New refinements and validation of the MODIS Land Surface Temperature / Emissivity products. Remote Sensing of Environment 112, 59-74, doi: 10.1016/j.rse.2006.06.02(2008)6.
11. Wan, Z. MODIS Land Surface Temperature Products Users' Guide. MODIS LST Products Technical Guide, 1-62, doi: 10.5067/MODIS/MOD11_L2.006(2014).
12. Bennouna, Y. S. et al., The evaluation of the integrated water vapour annual cycle over the Iberian Peninsula from EOS-MODIS against different ground-based techniques. Q. J. R. Meteorol. Soc. 139, 1935-1956, doi: 10.1002/qj.2080(2013).
13. Berk, A. et al., MODTRAN5: A reformulated atmospheric band model with auxiliary species and practical multiple scattering options. Proc. SPIE 5806, 662-667, doi: 10.1117/12.606026(2005).
14. Berk, A. et al., MODTRAN6: A major upgrade of the MODTRAN radiative transfer code. Proc. SPIE 9088, 90880H, doi: 10.1117/12.2050433(2014).
15. Wan, Z. & Dozier, J. A generalized split-window algorithm for retrieving land-surface temperature from space. IEEE Transactions on Geoscience and Remote Sensing 34, 892-905, doi: 10.1109/36.508406(1996).
16. Gao, B. C., Kaufman, Y. J. & Han, W. Correction of thin cirrus path radiances in the 0.4 – 1.0 μm spectral region using the MODIS cloud product. Journal of Geophysical Research: Atmospheres 103, 32169-32176, doi: 10.1029/98JD02006(1998).
17. Coll, C. et al., Ground measurements for the validation of land surface temperatures derived from AATSR and MODIS data. Remote Sensing of Environment 97, 288-300, doi: 10.1016/j.rse.2005.05.007(2005).
18. Mieruch, S. et al., Comparison of water vapor column amounts derived from GOME and MODIS measurements. Journal of Geophysical Research: Atmospheres 113, D19, doi: 10.1029/2008JD010000(2008).
19. NASA MODIS Land Team, MODIS Land Surface Temperature Products Users' Guide. Available from: https://lpdaac.usgs.gov (2015).
20. NASA Goddard Space Flight Center (GSFC), MODIS Atmosphere Water Vapor Product Overview. Available from: https://modis-atmos.gsfc.nasa.gov (2020).
21. Ndossi, M. I. & Avdan, U. Inversion of land surface temperature (LST) using Terra ASTER data: a comparison of three algorithms. Remote Sensing 8, 993, doi: 10.3390/rs8120993(2016).
22. Hersbach, H. et al., The ERA5 global reanalysis. Q. J. R. Meteorol. Soc. 146, 1999-2049, doi: 10.1002/qj.3803(2020).
23. Zhang, Y. L. et al., Consistency evaluation of precipitable water vapor derived from ERA5, ERA – Interim, GNSS, and radiosondes over China. Radio Science 54, 561-571, doi: 10.1029/2018RS006789(2019).
24. Ware, R. H. et al., SuomiNet: a real–time national GPS network for atmospheric research and education. Bulletin of the American Meteorological Society 81, 677-694, doi: 10.1175/1520-0477(2000)081<0677>2.3.CO;2(2000).